European Archives of Oto-Rhino-Laryngology (2019) 276:505–512
https://doi.org/10.1007/s00405-018-5231-x

HEAD & NECK

Amide proton transfer MRI detects early changes in nasopharyngeal carcinoma: providing a potential imaging marker for treatment response

Sahrish Qamar[1] · Ann D. King[1] · Qi-Yong Ai[1] · Benjamin King Hong Law[1] · Janet S. M. Chan[1] · Darren M. C. Poon[2] · Macy Tong[2] · Frankie Kwok Fai Mo[2] · Weitian Chen[1] · Kunwar S. Bhatia[3] · Anil T. Ahuja[1] · Brigette B. Y. Ma[2] · David Ka-Wai Yeung[2] · Yi-Xiang Wang[1] · Jing Yuan[4]

Received: 14 November 2018 / Accepted: 28 November 2018 / Published online: 3 December 2018

Abstract

Purpose To determine if treatment of nasopharyngeal carcinoma (NPC) induces early changes in amide proton transfer-weighted (APTw) magnetic resonance imaging (MRI), and to perform a preliminary evaluation of APTw imaging in response assessment.

Methods Sixteen patients with NPC planned for treatment with radiotherapy and/or chemotherapy underwent APTw imaging of the primary tumour pre-treatment and 2-week intra-treatment. Difference in pre- and intra-treatment APT mean (APT_{mean}) was compared using the Wilcoxon signed rank test. Differences in APT_{mean} and percentage change (%Δ) in APT_{mean} were compared between responders and non-responders based on the outcome at 6 months, using the Mann–Whitney *U* test.

Results APT_{mean} decreased in 9/16 (56.3%) and increased in 7/16 (43.7%) with no significant difference between the pre- and intra-treatment APT values for the whole group ($p > 0.05$). NPC showed response in 11/16 (68.8%) and non-response in 5/11 (31.2%). There were significant differences between the %Δ of responders and non-responders for APT_{mean} ($p = 0.01$). Responders showed %Δ decrease in APT_{mean} of −23.12% while non-responders showed a %Δ increase in APT_{mean} of +102.28%.

Conclusion APT value changes can be detected in early intra-treatment. Intra-treatment %Δ APT_{mean} shows potential in predicting short-term outcome.

Keywords Amide proton transfer-weighted imaging · Chemical exchange saturation transfer · Magnetic resonance imaging · Nasopharyngeal carcinoma · Treatment response

Introduction

Locoregional relapse remains an important determinant of failure in nasopharyngeal carcinoma (NPC) [1]. Functional magnetic resonance imaging (MRI) produces imaging biomarkers that may predict response and allow treatment regimens to be modified before or early in the course of

Electronic supplementary material The online version of this article (https://doi.org/10.1007/s00405-018-5231-x) contains supplementary material, which is available to authorized users.

✉ Ann D. King
king2015@cuhk.edu.hk

[1] Department of Imaging and Interventional Radiology, Faculty of Medicine, The Chinese University of Hong Kong, Prince of Wales Hospital, 30-32 Ngan Shing Street, Shatin, New Territories, Hong Kong S.A.R., China

[2] Department of Clinical Oncology, State Key Laboratory Translational Oncology, Faculty of Medicine, The Chinese University of Hong Kong, Prince of Wales Hospital, Shatin, New Territories, Hong Kong S.A.R., China

[3] Imaging Department, St Mary's Hospital, Imperial College Healthcare, National Health Service Trust, London, UK

[4] Medical Physics and Research Department, Hong Kong Sanatorium & Hospital, Happy Valley, Hong Kong S.A.R., China

treatment. Currently, diffusion-weighted imaging (DWI) is the most promising MRI technique in head and neck cancer, and the apparent diffusion coefficient (ADC) is the most widely reported parameter. Non-responding cancers tend to have a higher ADC before treatment and a lower % rise in ADC in the first few weeks of treatment, compared to responding head and neck cancer, including NPC [2–5]. However, there are still limitations to using DWI and no thresholds have been established [5].

Amide proton transfer-weighted (APTw) imaging [6], a subset of chemical exchange saturation transfer (CEST) imaging, has emerged as another promising MRI technique for assessing cancers and treatment response. Increased tumour cellularity is associated with an increase in abnormal protein synthesis and overexpression of several proteins and peptides which are rich in amide protons [7], and in brain cancer a positive correlation has been observed between APT values and cellularity [8–11]. Early research into a range of cancers in the brain, breast, prostate, rectum and lungs suggests APT values may be able to characterize or grade cancers [9, 10, 12–21], differentiate cancers from post-treatment changes [22, 23] and assess treatment response [8, 24–29]. There is a paucity of research on APTw imaging in the head and neck but early reports show APT values are higher in tumours compared to normal surrounding tissues [30, 31]. To the best our knowledge, it is unknown if treatment induces early changes in head and neck cancer APT values and if so whether early intra-treatment changes predict treatment response.

The primary aim of this preliminary study was to determine if APTw imaging is able to detect changes in APT early in the course of treatment of NPC. The secondary aim was to correlate APT values and change in APT values with short-term outcome.

Materials and methods

Subjects

This prospective study received approval from the local institutional ethics committee and written informed consent was obtained from all patients. From March, 2016 to September, 2017, 16 patients, with newly diagnosed biopsy-proven undifferentiated NPC with a primary tumour ≥ 1 cm, planned for treatment with radiotherapy and/or chemotherapy were recruited for the study. Three patients have been reported in a previous tumour characterisation study which did not evaluate treatment changes [31].

CEST acquisition and processing

MRI was performed pre-treatment and intra-treatment at 2 weeks after the start of treatment, on a Philips Achieva TX 3T scanner (Philips Healthcare, Best, The Netherlands) using body coil for radiofrequency pulse transmission and a Philips neurovascular phased-array coil for reception for head and neck imaging. Conventional anatomical images included T1w and T2w with fat saturation; in addition, T1w contrast-enhanced images were obtained on the pre-treatment scan. The largest cross-section of solid primary tumour was selected for single-slice APTw imaging. APTw imaging used a single-selection turbo spin-echo sequence with chemical shift-selective fat suppression (slice thickness = 4 mm; field of view = 230 × 230 mm; voxel size 2 × 2 mm; TE = 8 ms; TR = 2000 ms; echo train length = 14; number of signal average = 1; sensitivity encoding SENSE factor = 2; flip angle = 90° and partial Fourier factor = 0.7). To minimize ΔB_0 inhomogeneity localized high-order shimming was executed. A continuous rectangular radiofrequency pulse with the B_1 field strength of 2 µT and a fixed time of duration of 200 ms (× 4) was used for saturation. First, a baseline image without applying the saturation pulse was acquired and then the saturated images were acquired at the frequency offsets of ± 0.25, ± 0.5, ± 1, ± 1.5, ± 2, ± 2.5, ± 3, ± 3.5, ± 4, ± 4.5, ± 5, ± 5.5, ± 6.5, ± 7.5 ppm. The saturation images at positive and negative offsets were acquired in an interleaved fashion. The scan time for APTw imaging was approximately 1 min 40 s. Details of processing and z spectrum analysis of APTw imaging data can be found in the past studies [30, 31]. MTR_{asym} (magnetization transfer ratio asymmetry) measured at the offset of 3.5 ppm produced the APTw image.

CEST analysis

Using the anatomical images for correlation, the area of the single representative slice through the primary tumour was contoured manually excluding necrotic areas on both pre-treatment and intra-treatment APTw images. The primary tumour was contoured by one observer twice (1 month apart) with 23 years of experience and by a second observer with 4 years of experience in MRI of the head and neck. The APT mean (APT_{mean}) was extracted from histogram analysis of the pre-treatment and intra-treatment APTw images, and APT_{mean} absolute change (Δ) between the two time points and % change (%Δ) [(intra-treatment measurement − pre-treatment measurement)/pre-treatment measurement × 100] were calculated. The volume of the primary tumour was obtained pre-treatment

and intra-treatment by manually outlining the area on each slice and multiplying the sum of the areas by the slice thickness. The Δ and %Δ in volume were calculated as described for the APT_{mean} above.

Study endpoint

The short-term outcome of NPC was evaluated at 6 months after the end of treatment. Patients were designated as locoregional non-responders if they had histologically confirmed residual NPC, an enlarging residual mass, or a residual mass at the end of treatment which received an additional radiotherapy boost. All other patients were designated as locoregional responders.

Statistical analysis

Intraclass correlation coefficients (ICC) were calculated to assess intra-observer and inter-observer agreement for APT_{mean}. The median values for APT_{mean}, and volume pre-treatment and intra-treatment were compared using the Wilcoxon signed rank tests for non-parametric data. Afterwards, these parameters and changes in these parameters (Δ and %Δ) were compared between responders and non-responders using the Mann–Whitney *U* tests. Statistical analysis was performed using SPSS software (v24.0, IBM, Armonk, NY). All statistical tests were two sided, and a *p* value of less than 0.05 was considered to indicate a statistically significant difference.

Results

Patients

APTw imaging was successful in all 16 NPC patients (male:female = 13:3; mean age = 49.4 ± 9.9 years (range 36–67 years) and tumour shortest diameter = 1.84 ± 0.42 cm). The time interval between the treatment initiation and intra-treatment scan was 14.5 ± 4.3 (12–29) days. At 6 months post-treatment, 5/16 (31.2%) NPCs were non-responders based on a positive biopsy at the primary site ($n = 2$), an enlarging primary tumour ($n = 1$) and a residual nodal mass requiring a radiotherapy boost ($n = 2$), the remaining 11/16 (68.8%) were responders. The tumour characteristics with respective $\%\Delta APT_{mean}$ are shown in Table 1.

Intra and inter-observer agreement

The intra and inter-observer agreement ICC showed good to excellent agreement ($p < 0.05$) at 95% confidence interval (Supplementary Table 1) and the averaged values between inter-observer measurement and the average of intra-observer measurements were used in this study.

Differences in APT_{mean}, and volume between pre- and intra-treatment for the whole group

Pre-treatment and intra-treatment APT_{mean} of the whole group showed no statistical difference between the two

Table 1 Tumour characteristics, treatment and intra-treatment $\%\Delta APT_{mean}$ of NPC patients

Patient no.	Overall stage[a]	Treatment	Diameter (cm)	Outcome	$\%\Delta APT_{mean}$
1	III	CCRT	1.57	Responder	−51.96
2	II	CCRT	2.37	Responder	−31.64
3	III	CCRT	1.74	Non-responder	49.49
4	IV	CCRT	1.39	Responder	−27.36
5	II	CCRT	1.36	Responder	−23.12
6	IV	CCRT	1.25	Responder	−17.93
7	IV	CCRT	1.41	Non-responder	102.28
8	III	CCRT	1.98	Responder	38.32
9	IV	CCRT	2.79	Responder	−31.41
10	IV	CCRT	1.90	Responder	−61.43
11	II	CCRT	1.73	Non-responder	−20.08
12	III	CCRT	2.12	Non-responder	463.33
13	III	CCRT	1.62	Responder	49.50
14	IV	Palliative chemotherapy	2.22	Non-responder	249.91
15	III	CCRT	2.10	Responder	14.68
16	IV	NAC + CCRT	1.88	Responder	−8.96

NPC Nasopharyngeal carcinoma, *CCRT* concurrent chemoradiotherapy, *NAC* neoadjuvant chemotherapy, $\%\Delta APT_{mean}$ % change in APT mean

[a]NPC staging was according to the 7th edition of the Union for International Cancer Control (UICC)

Table 2 APT_{mean}, and volume of pre-treatment and intra-treatment for the whole group of 16 NPC patients

	Pre-treatment median (range)	Intra-treatment median (range)	*z* (*p* value)
APT_{mean} (%)	2.41 (0.26–4.11)	2.50 (0.58–3.63)	− 0.310 (0.756)
Volume (cm^3)	102.05 (29.0–432.0)	51.55 (10.10–345.6)	− 3.516 (< 0.001)

APT Amide proton transfer, APT_{mean} APT mean, *z* Wilcoxon signed ranked test statistic

Table 3 APT_{mean}, volume pre-treatment and intra-treatment, and change (Δ and %Δ) for responders and non-responders

	Responders median (range)	Non-responders median (range)	*z* (*p* value)
APT_{mean} (%)			
Pre-treatment	2.67 (1.21–4.11)	1.50 (0.26–2.92)	− 1.53 (0.13)
Intra-treatment	2.50 (0.58–3.37)	2.59 (1.45–3.63)	− 0.74 (0.46)
ΔAPT_{mean}	− 0.63 (− 2.37 to 0.90)	1.20 (− 0.59 to 1.85)	− 2.66 (0.01)
$\%\Delta APT_{mean}$	− 23.12 (− 61.43 to 49.50)	102.28 (− 20.08 to 463.33)	− 2.44 (0.01)
Volume (cm^3)			
Pre-treatment	106.2 (31.4–321.0)	67.6 (29.0–432.0)	− 0.40 (0.69)
Intra-treatment	49.0 (10.1–279.0)	52.0 (21.9–345.6)	− 0.62 (0.53)
Δ Volume	− 42.0 (− 110.5 to − 2.0)	− 12.0 (− 86.4 to − 7.10)	− 0.74 (0.46)
%Δ Volume	− 35.6 (− 6.30 to − 87.0)	− 20.0 (− 11.6 to − 54.80)	− 0.96 (0.34)

APT Amide proton transfer, APT_{mean} APT mean, *Δ* absolute change, *%Δ* relative change, *z* Mann–Whitney *U* test statistic

time points ($p > 0.05$) (Table 2). A decrease in APT_{mean} (range: − 8.96 to − 61.43%) was observed in 9/16 (56.3%) while an increase in APT_{mean} (range 14.68–463.33%) was observed in 7/16 (43.7%) cases. Pre- and intra-treatment volumes of the whole group showed a statistically significant decrease between the pre- and intra-treatment scans ($p < 0.001$) (Table 2).

Differences in APT_{mean}, and volume between responders and non-responders

The pre- and intra-treatment APT_{mean} and volume, and the Δ and %Δ in these parameters, for responders and non-responders, are shown in Table 3. APT_{mean} showed higher pre-treatment and lower intra-treatment values for responders compared to non-responders, but statistical significance was not reached ($p > 0.05$). The Δ and %Δ APT_{mean} showed a significant decrease in responders and a significant increase in non-responders ($p = 0.01$). Figure 1 shows the box plot of %Δ for responders and non-responders, and Fig. 2 shows the normalized %Δ APT_{mean} with the reference line normalized to a mean value 0 for all 16 NPC cases. An example of a responder and non-responder are shown in Figs. 3 and 4, respectively. Primary tumour volume pre-treatment, intra-treatment, Δ and %Δ showed no significant difference between responders and non-responders (all $p > 0.05$) (Table 3).

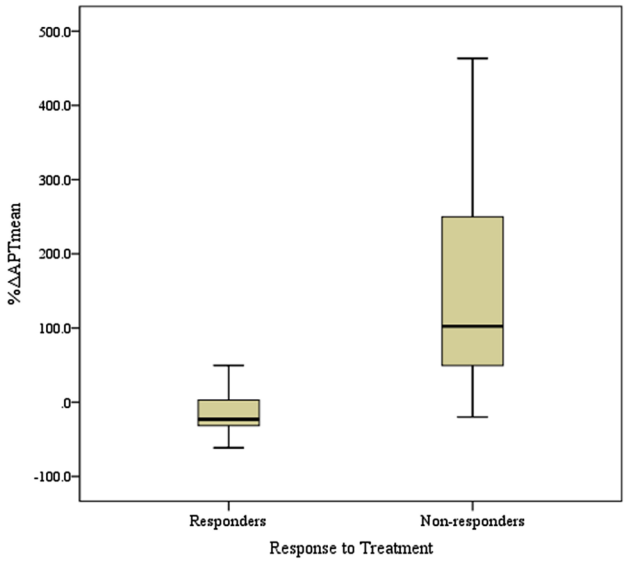

Fig. 1 Boxplot of $\%\Delta APT_{mean}$ at 2 weeks of treatment for responding and non-responding NPCs. Responders tended to show decreasing APT_{mean} and non-responders tended to show increasing APT_{mean}

Discussion

APTw imaging is a new MRI technique for examining cancer and its role in treatment response assessment of head and neck cancer is unknown. Therefore, in the first part of the study we aimed to determine if APTw imaging could detect early changes in the NPC and we found that in all

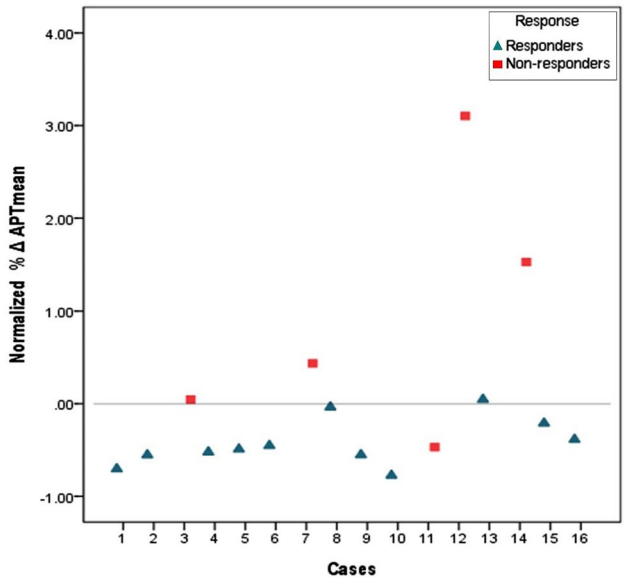

Fig. 2 Normalized values of %Δ APT_{mean} between responders and non-responders. Majority of responders were below and non-responders were above the normalized baseline at 0 representing decreasing and increasing %Δ APT_{mean}, respectively. All results were within ±2 standard deviations of the baseline with the exception of one outlier that showed non-response

cases a change in APT level was detectable by 2 weeks after the start of treatment.

We expected treatment-induced cell death would decrease protein synthesis and the overexpression of proteins and peptides rich in amide protons, leading to a decrease in APT values. However, the changes were mixed with just over half of our cases showing the expected decrease while the remainder showed an increase in APT value. Because of the mixed change, there was no statistical difference in the APT values between pre-treatment and intra-treatment in the whole group of tumours. A similar mixed change with both an increase and decrease in APT levels has been reported in two early breast cancer studies [24, 26]. These two studies in patients treated by chemotherapy observed a ratio of decreasing:increasing APT levels of 7:3 early intra-treatment [26] and 2:1 post-treatment [24].

In the second part of this study, we did a preliminary analysis of APT values to determine if the mixed changes we observed in APT values could be caused by differences in treatment response. We found the change in APT_{mean} 2 weeks after the start of treatment was significantly different between responders and non-responders, based on the short-term outcome at 6 months. The decrease in APT_{mean}

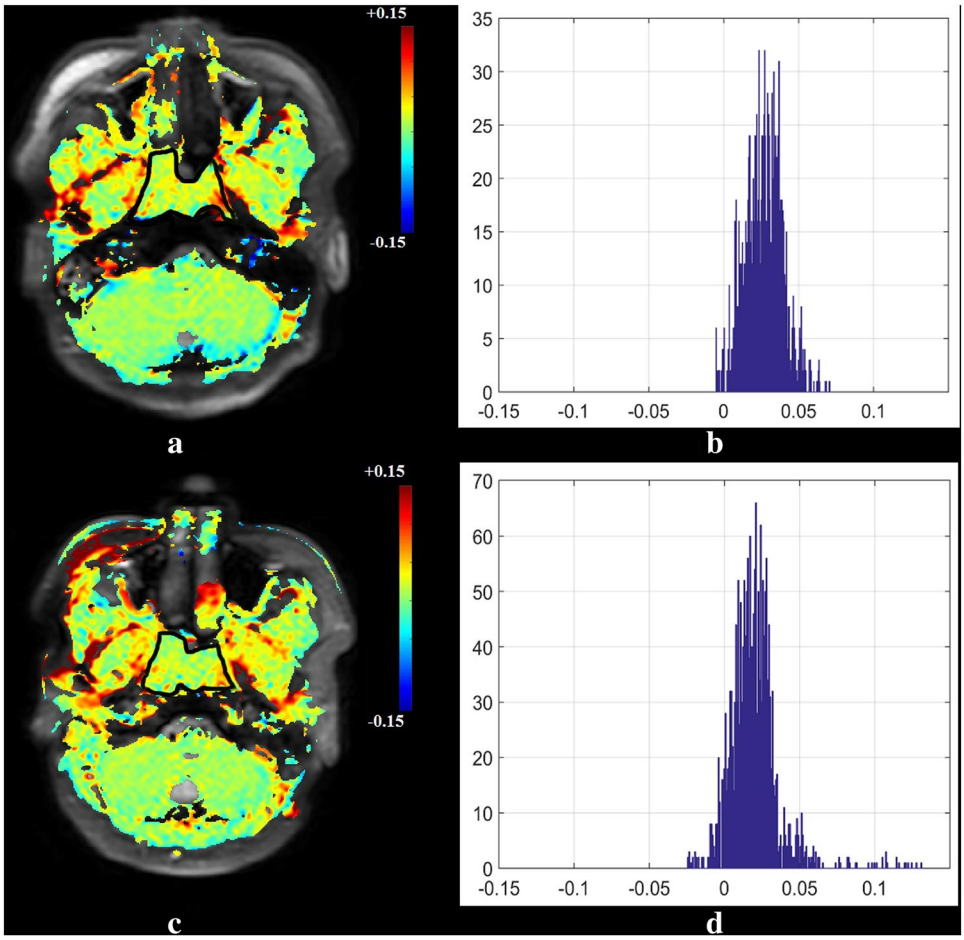

Fig. 3 52-Year-old male with a histologically confirmed responding nasopharyngeal carcinoma. Pre-treatment **a** axial APTw image and **b** APT histogram. Intra-treatment **c** axial APTw image and **d** APT histogram. The APT_{mean} decreased from 2.67% pre-treatment to 2.05% intra-treatment (%Δ $APT_{mean} = -23.12\%$)

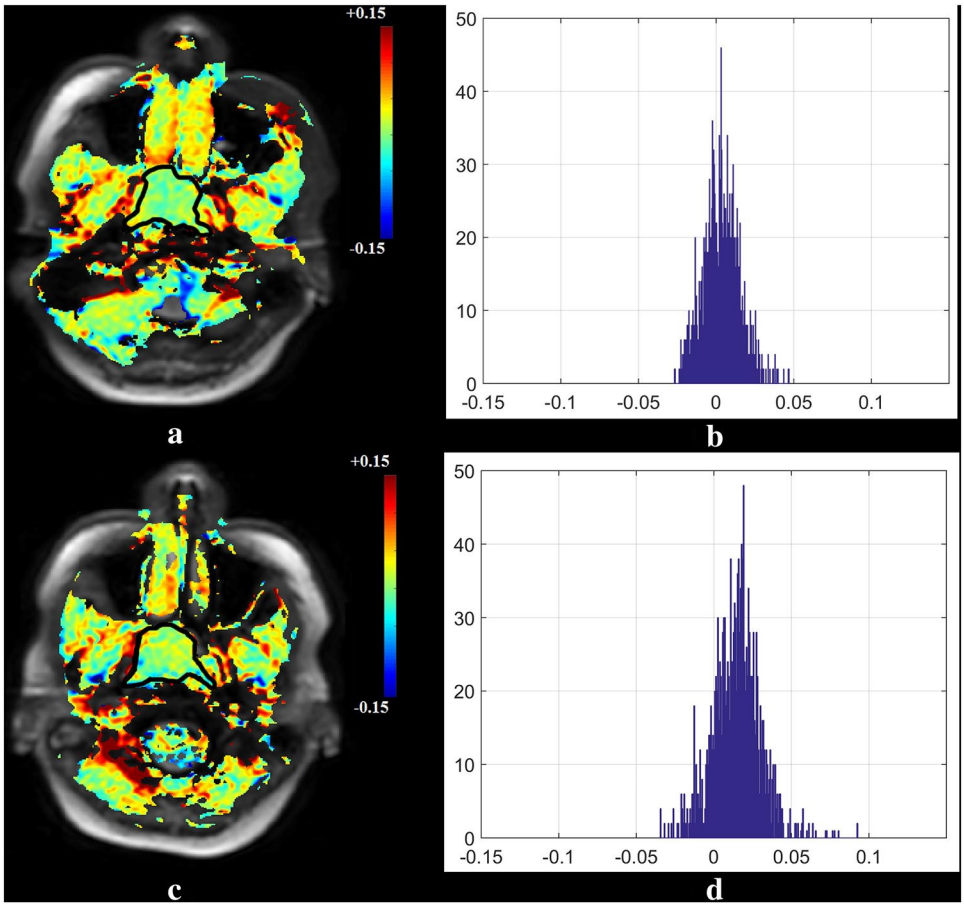

Fig. 4 36-Year-old female with a histologically confirmed non-responding nasopharyngeal carcinoma. Pre-treatment **a** axial APTw image and **b** APT histogram. Intra-treatment **c** axial APTw image and **d** APT histogram. APT_{mean} increased from pre-treatment 0.26% to intra-treatment 1.45% (%Δ $APT_{mean} = +463.3\%$)

was smaller in non-responders compared to responders and interestingly most of the non-responders showed an increase in APT_{mean}. A similar intra-treatment increase in APT values at 1–2 weeks in tumours with an unfavorable response has been observed also in glioblastoma [8] and breast cancer [24]. The pathophysiological explanation for this early intra-treatment increase in APT values is unknown but one possibility is that it may be due to an early proliferation of resistant tumour cells.

The preliminary results from our study and previous studies in other cancer groups suggest that rising APT values could be an early imaging marker of poor response so allowing treatment to be modified. For head and neck cancer, in the future this potentially could allow for the escalation of radiotherapy using dose painting or the addition of target agents. However, a minority of responders in our study and in a previously reported breast cancer study [26] also showed increasing APT values. Therefore, the mechanisms underlying changes in APT values are likely to be far more complex than currently understood and could involve factors such as intratumoural pH changes, the influence of which on APTw imaging is still unclear [24, 27].

This study has some limitations. First, because this was a preliminary study the sample size was small, and we choose only to examine tumours > 1 cm. Therefore, we did not attempt to calculate the diagnostic performance of APTw imaging, and the success rate in obtaining APTw images may be higher than that in a general population which includes patients with smaller primary tumours. Second, we only examined the association of APTw imaging with short-term outcome and one of the indicators of short-term non-response, a residual mass requiring a radiotherapy boost, was based on the clinical judgment of the radiotherapist. Third, current constraints in APTw imaging only allow the examination of one slice through the tumour which may not be representative of the APT value in very heterogeneous tumours.

Conclusions

In summary, APTw imaging could detect changes in APT_{mean} in primary NPC 2 weeks after the start of treatment, and both an increase and a decrease in APT_{mean} were observed. Compared to responding tumours, non-responding tumours tended to show an increase, rather than a decrease, in APT_{mean}. This is one of the first studies to assess treatment-induced APT changes in head and neck cancer, and

although it is only a preliminary study the results are encouraging and suggest APTw imaging may have a valuable role in treatment assessment.

Acknowledgements The authors thank Dr Jinyuan Zhou, Department of Radiology, Johns Hopkins University, for providing technical advice on pulse sequencing.

Funding The work described in this paper was supported by grants from the Research Grants council of the Hong Kong Special Administrative Region, China (Project no. CUHK141070/14 and SEG_CUHK02).

Compliance with ethical standards

Conflict of interest The authors declare that they have no conflict of interest.

Ethical approval All procedures performed in studies involving human participants were in accordance with the ethical standards of the institutional and/or national research committee and with the 1964 Helsinki declaration and its later amendments or comparable ethical standard.

Informed consent Informed consent was obtained from all individual participants included in the study.

References

1. Li L, Huang S, Zhu X, Zhou Z, Liu Y, Qu S, Guo Y (2013) Identification of radioresistance-associated proteins in human nasopharyngeal carcinoma cell lines by proteomic analysis. Cancer Biother Radiopharm 28(5):380–384
2. Chen Y, Liu X, Zheng D, Xu L, Hong L, Xu Y, Pan J (2014) Diffusion-weighted magnetic resonance imaging for early response assessment of chemoradiotherapy in patients with nasopharyngeal carcinoma. Magn Reson Imaging 32(6):630–637
3. Hong J, Yao Y, Zhang Y, Tang T, Zhang H, Bao D, Chen Y, Pan J (2013) Value of magnetic resonance diffusion-weighted imaging for the prediction of radiosensitivity in nasopharyngeal carcinoma. Otolaryngol Head Neck Surg 149(5):707–713
4. Thoeny HC, Keyzer FD, King AD (2012) Diffusion-weighted MR imaging in the head and neck. Radiology 263(1):19–32
5. King AD, H.C (2016) Thoeny, functional MRI for the prediction of treatment response in head and neck squamous cell carcinoma: potential and limitations. Cancer Imaging 16(1):23
6. Zhou J, Lal B, Wilson DA, Laterra J, van Zijl PC (2003) Amide proton transfer (APT) contrast for imaging of brain tumors. Magn Reson Med 50(6):1120–1126
7. Cairns RA, Harris IS, Mak TW (2011) Regulation of cancer cell metabolism. Nat Rev Cancer 11(2):85–95
8. Sagiyama K, Mashimo T, Togao O, Vemireddy V, Hatanpaa KJ, Maher EA, Mickey BE, Pan E, Sherry AD, Bachoo R, Takahashi M (2014) In vivo chemical exchange saturation transfer imaging allows early detection of a therapeutic response in glioblastoma. Proc Natl Acad Sci USA 111(12):4542–4547
9. Bai Y, Lin Y, Zhang W, Kong L, Wang L, Zuo P, Vallines I, Schmitt B, Tian J, Song X, Zhou J, Wang M (2017) Noninvasive amide proton transfer magnetic resonance imaging in evaluating the grading and cellularity of gliomas. Oncotarget 8(4):5834–5842
10. Togao O, Yoshiura T, Keupp J, Hiwatashi A, Yamashita K, Kikuchi K, Suzuki Y, Suzuki SO, Iwaki T, Hata N, Mizoguchi M, Yoshimoto K, Sagiyama K, Takahashi M, Honda H (2014) Amide proton transfer imaging of adult diffuse gliomas: correlation with histopathological grades. Neuro Oncol 16(3):441–448
11. Jiang S, Eberhart CG, Zhang Y, Heo HY, Wen Z, Blair L, Qin H, Lim M, Quinones-Hinojosa A, Weingart JD, Barker PB, Pomper MG, Laterra J, van Zijl PCM, Blakeley JO, Zhou J (2017) Amide proton transfer-weighted magnetic resonance image-guided stereotactic biopsy in patients with newly diagnosed gliomas. Eur J Cancer 83:9–18
12. Takayama Y, Nishie A, Togao O, Asayama Y, Ishigami K, Ushijima Y, Okamoto D, Fujita N, Sonoda K, Hida T, Ohishi Y, Keupp J, Honda H (2018) Amide proton transfer MR imaging of endometrioid endometrial adenocarcinoma: association with histologic grade. Radiology 286(3):909–917
13. Takayama Y, Nishie A, Sugimoto M, Togao O, Asayama Y, Ishigami K, Ushijima Y, Okamoto D, Fujita N, Yokomizo A, Keupp J, Honda H (2016) Amide proton transfer (APT) magnetic resonance imaging of prostate cancer: comparison with Gleason scores. MAGMA 29(4):671–679
14. Sakata A, Okada T, Yamamoto Y, Fushimi Y, Dodo T, Arakawa Y, Mineharu Y, Schmitt B, Miyamoto S, Togashi K (2018) Addition of amide proton transfer imaging to FDG-PET/CT improves diagnostic accuracy in glioma grading: a preliminary study using the continuous net reclassification analysis. AJNR Am J Neuroradiol 39(2):265–272
15. Jia G, Abaza R, Williams JD, Zynger DL, Zhou J, Shah ZK, Patel M, Sammet S, Wei L, Bahnson RR, Knopp MV (2011) Amide proton transfer MR imaging of prostate cancer: a preliminary study. J Magn Reson Imaging 33(3):647–654
16. Ohno Y, Yui M, Koyama H, Yoshikawa T, Seki S, Ueno Y, Miyazaki M, Ouyang C, Sugimura K (2016) Chemical exchange saturation transfer MR imaging—preliminary results for differentiation of malignant and benign thoracic lesions. Radiology 279(2):578–589
17. Dula AN, Dewey BE, Arlinghaus LR, Williams JM, Klomp D, Yankeelov TE, Smith S (2015) Optimization of 7-T chemical exchange saturation transfer parameters for validation of glycosaminoglycan and amide proton transfer of fibroglandular breast tissue. Radiology 275(1):255–261
18. Zhang J, Zhu W, Tain R, Zhou XJ, Cai K (2018) Improved differentiation of low-grade and high-grade gliomas and detection of tumor proliferation using APT contrast fitted from Z-spectrum. Mol Imaging Biol 20(4):623–631
19. Zhou J, Blakeley JO, Hua J, Kim M, Laterra J, Pomper MG, van Zijl PC (2008) Practical data acquisition method for human brain tumor amide proton transfer (APT) imaging. Magn Reson Med 60(4):842–849
20. Zhou J, Zhu H, Lim M, Blair L, Quinones-Hinojosa A, Messina SA, Eberhart CG, Pomper MG, Laterra J, Barker PB, van Zijl PC, Blakeley JO (2013) Three-dimensional amide proton transfer MR imaging of gliomas: Initial experience and comparison with gadolinium enhancement. J Magn Reson Imaging 38(5):1119–1128
21. Jiang S, Yu H, Wang X, Lu S, Li Y, Feng L, Zhang Y, Heo HY, Lee DH, Zhou J, Wen Z (2016) Molecular MRI differentiation between primary central nervous system lymphomas and high-grade gliomas using endogenous protein-based amide proton transfer MR imaging at 3 T. Eur Radiol 26(1):64–71
22. Park KJ, Kim HS, Park JE, Shim WH, Kim SJ, Smith SA (2016) Added value of amide proton transfer imaging to conventional and perfusion MR imaging for evaluating the treatment response of newly diagnosed glioblastoma. Eur Radiol 26(12):4390–4403
23. Zhou J, Tryggestad E, Wen Z, Lal B, Zhou T, Grossman R, Wang S, Yan K, Fu DX, Ford E, Tyler B, Blakeley J, Laterra J, van Zijl PC (2011) Differentiation between glioma and radiation necrosis using molecular magnetic resonance imaging of endogenous proteins and peptides. Nat Med 17(1):130–134

24. Dula AN, Arlinghaus LR, Dortch RD, Dewey BE, Whisenant JG, Ayers GD, Yankeelov TE, Smith SA (2013) Amide proton transfer imaging of the breast at 3 T: establishing reproducibility and possible feasibility assessing chemotherapy response. Magn Reson Med 70(1):216–224
25. Jing Z, Yinsheng C, Yiying Z, Shasha Y, Zhongping C, Yin W (2017) Assessment of chemoradiotherapy response in glioma with magnetic resonance amide proton transfer imaging in a rodent model. Conf Proc IEEE Eng Med Biol Soc 2017:541–543
26. Krikken E, Khlebnikov V, Zaiss M, Jibodh RA, van Diest PJ, Luijten PR, Klomp DWJ, van Laarhoven HWM, Wijnen JP (2018) Amide chemical exchange saturation transfer at 7 T: a possible biomarker for detecting early response to neoadjuvant chemotherapy in breast cancer patients. Breast Cancer Res 20(1):51
27. Nishie A, Asayama Y, Ishigami K, Ushijima Y, Takayama Y, Okamoto D, Fujita N, Tsurumaru D, Togao O, Sagiyama K, Manabe T, Oki E, Kubo Y, Hida T, Hirahashi-Fujiwara M, Keupp J, Honda H (2018) Amide proton transfer imaging to predict tumor response to neoadjuvant chemotherapy in locally advanced rectal cancer. J Gastroenterol Hepatol. https://doi.org/10.1111/jgh.14315
28. Hong X, Liu L, Wang M, Ding K, Fan Y, Ma B, Lal B, Tyler B, Mangraviti A, Wang S, Wong J, Laterra J, Zhou J (2014) Quantitative multiparametric MRI assessment of glioma response to radiotherapy in a rat model. Neuro Oncol 16(6):856–867
29. Ma B, Blakeley JO, Hong X, Zhang H, Jiang S, Blair L, Zhang Y, Heo HY, Zhang M, van Zijl PC, Zhou J (2016) Applying amide proton transfer-weighted MRI to distinguish pseudoprogression from true progression in malignant gliomas. J Magn Reson Imaging 44(2):456–462
30. Yuan J, Chen S, King AD, Zhou J, Bhatia KS, Zhang Q, Yeung DK, Wei J, Mok GS, Wang YX (2014) Amide proton transfer-weighted imaging of the head and neck at 3 T: a feasibility study on healthy human subjects and patients with head and neck cancer. NMR Biomed 27(10):1239–1247
31. Law BKH, King AD, Ai QY, Poon DMC, Chen W, Bhatia KS, Ahuja AT, Ma BB, Ka-Wai D, Yeung FK, Fai Mo YX, Wang J, Yuan (2018) Head and neck tumors: amide proton transfer MRI. Radiology 288(3):782–790